Monitoring Cardiovascular Physiology using Bio-compatible AlN Piezoelectric Skin Sensors

Date of publication xxxx 00, 0000, date of current version xxxx 00, 0000.

Digital Object Identifier 10.1109/ACCESS.2017.DOI

Monitoring Cardiovascular Physiology using Bio-compatible AlN Piezoelectric Skin Sensors

ANGELA TAFADZWA SHUMBA[1,1,2,*],(Graduate Student Member, IEEE), SULEYMAN MAHIRCAN DEMIR[†,1,3,*],(Graduate Student Member, IEEE), VINCENZO MARIANO MASTRONARDI[1,2], FRANCESCO RIZZI[1], GAIA DE MARZO[1], LUCA FACHECHI[1], PAOLO MOTTO ROS[3],(Member, IEEE), DANILO DEMARCHI[3],(Senior Member, IEEE), LUIGI PATRONO[2], (Member, IEEE) MASSIMO DE VITTORIO[1,2],(Senior Member, IEEE)

[1]Centre for Biomolecular Nanotechnologies, Istituto Italiano di Tecnologia, Arnesano, Italy
[2]Department of Engineering for Innovation, University of Salento, Lecce, Italy
[3]Department of Electronics and Telecommunications, Politecnico di Torino, Turin, Italy
[*]Authors to whom correspondence should be addressed
[†]Both authors are considered first authors.

Corresponding authors: Angela T. Shumba (e-mail: angela.shumba@iit.it). Suleyman M. Demir (e-mail: mahircan.demir@iit.it)

This research is funded by Progetto "RAISE (Robotics and AI for Socio-economic Empowerment)" ECS00000035 supported by European Union - NextGenerationEU PNRR MUR - M4C2 – I1.5 - Avviso "Ecosistemi dell'Innovazione" and by Progetto "SOMNIIA MONITOR" (Contratto ASI n. 2023-7-U.0 "SOMNIIA MONITOR: poliSOnnigrafo Multi-sensore Non-Invasivo Indossabile per Astronauti con MONITOraggio Remoto dei parametri vitali e della qualità del sonno"). However, the views and opinions expressed are those of the authors alone and do not necessarily reflect those of the European Union or the European Commission. Neither the European Union nor the European Commission can be held responsible for them.

ABSTRACT Arterial pulse waves contain a wealth of parameters indicative of cardiovascular disease. As such, monitoring them continuously and unobtrusively can provide health professionals with a steady stream of cardiovascular health indices, allowing for the development of efficient, individualized treatments and early cardiovascular disease diagnosis solutions. Blood pulsations in superficial arteries cause skin surface deformations, typically undetectable to the human eye; therefore, Microelectromechanical systems (MEMS) can be used to measure these deformations and thus create unobtrusive pulse wave monitoring devices. Miniaturized ultrathin and flexible Aluminium Nitride (AlN) piezoelectric MEMS are highly sensitive to minute mechanical deformations, making them suitable for detecting the skin deformations caused by cardiac events and consequently providing multiple biomarkers useful for monitoring cardiovascular health and assessing cardiovascular disease risk. Conventional wearable continuous pulse wave monitoring solutions are typically large and based on technologies limiting their versatility. Therefore, we propose the adoption of 29.5 μm-thick biocompatible, skin-conforming devices on piezoelectric AlN to create versatile, multipurpose arterial pulse wave monitoring devices. In our initial trials, the devices are placed over arteries along the wrist (radial artery), neck (carotid artery), and suprasternal notch (on the chest wall and close to the ascending aorta). We also leverage the mechano-acoustic properties of the device to detect heart muscle vibrations corresponding to heart sounds S1 and S2 from the suprasternal notch measurement site. Finally, we characterize the piezoelectric device outputs observed with the cardiac cycle events using synchronized electrocardiogram (ECG) reference signals and provide information on heart rate, breathing rate, and heart sounds. The extracted parameters strongly agree with reference values as illustrated by minimum Pearson correlation coefficients (r) of 0.81 for pulse rate and 0.95 for breathing rate

INDEX TERMS AlN thin films, Biocompatible, Cardiovascular disease, Heart rate, Heart sounds, MEMS, Piezoelectric, Phonocardiogram (PCG), Pulse waves, Skin sensors.

I. INTRODUCTION

CARDIOVASCULAR diseases (CVDs) are a group of heart and blood vessel disorders causing approximately 17 million annual global deaths [1]–[3]. According to the World Health Organization (WHO), out of all deaths recorded in 2019, CVDs were responsible for 38% of premature deaths and 32% of all fatalities [3]. Additionally, 80% of CVD-related deaths recorded annually are caused by heart attacks and strokes typically brought on by unhealthy lifestyles and sedentary behavior [3]. Therefore, research conducted towards reducing the global effects of CVDs revealed that continuously monitoring heart function and physical activity can be used to identify high-risk individuals and contribute to developing efficient CVD prevention measures and treatment plans [1], [4], [5]. Some methods typically used by medical practitioners to diagnose and assess the progression of CVDs include coronary computed tomography (CT) angiography, auscultation, echocardiography, electrocardiography, phonocardiography, and several other blood chemistry assessment methods [6]–[9]. These methods provide signals or images that can be used to assess and detect abnormalities in the structure or function of the heart and blood vessels to determine the presence of a CVD [10]–[13]. However, the equipment required is either costly, only accessible in specialized facilities, or operable only by well-trained personnel, thus limiting CVD assessment to infrequent hospital visits. Additionally, individuals who perceive themselves healthy are less likely to undergo the more specialized tests as they are expensive and may be considered unnecessary.

Low-cost, highly accessible, and easy-to-use devices that produce information identical to or compatible with these traditional techniques can, therefore, help keep people informed on their health status. These devices can also provide long-term patient data to help medical professionals make more informed decisions, facilitating more accurate CVD-related assessments [14]. As a result, developing low-cost, non-invasive technologies capable of providing parameters useful for monitoring pulse waves for CVD screening, prevention, and treatment has been the focus of several research studies [7], [15]. Portable and remote pulse wave monitoring devices for CVD screening and assessment, such as wearable electrocardiogram (ECG) devices, portable handheld ultrasound dopplers, and wearable devices based on photoplethysmography (PPG) have been developed to enable non-invasive remote cardiac assessment. However, many of these commercially available devices are still cumbersome, sometimes hard to use, and interfere with daily life activities, spurring the need for more unobtrusive, flexible, and smaller alternatives based on flexible electronics and MEMS [14], [16], [17]. As a result, monitoring heart function using MEMS devices that leverage the piezoelectric, capacitive, or piezoresistive effect is rapidly gaining popularity [14], [18], [19]. However, compared to piezoresistive or capacitive devices, piezoelectric transducers do not require any external power to function, making them more suitable for developing minimal bulk solutions [14]. Piezoelectric sensors also attract considerable attention since they enable the development of stable, precise, and flexible devices [20]. Additionally, AlN is one of the most popular piezoelectric materials thanks to its CMOS compatibility, thermal, mechanical, and chemical stability, good acoustic properties, and non-toxic nature [21]–[25]. This work, therefore, contributes to the research towards unobtrusive MEMS for continuous CVD screening and assessment by demonstrating bio-compatible AlN thin-film piezoelectric skin sensors for the extraction of heart rhythm, heart sounds, and respiration information from pulse waves detected from various on-body measurement sites.

Our main contributions are summarized as follows:

- We validate the potential of using AlN thin films to create continuous cardiovascular monitoring devices by extracting multiple essential physiological parameters critical for CVD diagnosis, risk definition, and patient monitoring from detected pulse waves.
- We analyze pulse wave signals obtained from several superficial arteries and provide a qualitative analysis of the piezoelectric pulse waves that provide physiological signals, including heart rate (HR), breathing rate (BR), and heart sounds.
- We comprehensively characterize the information embedded within the signals collected from each measurement site and validate the extracted physiological parameters using simultaneously collected ECG reference signals.

The paper is organized as follows: Section II reviews related works describing the application of AlN piezoelectric devices to obtain signals that allow the estimation of physiological parameters critical for CVD diagnosis and management. The experimental materials and methods are presented in Section III. Section IV discusses the results, and finally, conclusions, future perspectives, and recommendations are provided in Section V.

II. RELATED WORKS

As previously mentioned, AlN-based piezoelectric sensors are in great demand for many reasons, such as CMOS compatibility, non-toxicity, and good acoustic properties. As a result, some researchers have investigated the design and development of MEMS structures based on AlN for several healthcare applications [26]. For example, [27] presented an AlN piezoelectric sensor to measure pulse waves and employ the proposed sensor to monitor pulse waves from three different body positions: carotid, wrist, and clavicle. In addition, pulse waves from the carotid artery and ECG signals are recorded simultaneously to demonstrate their correlation. The paper provides pulse wave recordings; however, the correlation between the recorded pulse wave signals and physiological parameters is not provided. Natta et al. [28] described a soft and flexible piezoelectric smart patch based on AlN thin film used to monitor vascular grafts. The sensor was wrapped around a graft and tested *in-vitro* to measure

real-time variations of hemodynamic parameters. The authors obtained high sensitivity for real-time vascular graft monitoring. However, the same performance could not be achieved *in-vivo* due to electromagnetic interference (EMI) and the capacitive coupling occurring when the sensor is in contact with the skin. These effects introduce substantial noise, causing a significant decrease in signal-to-noise ratio.

On the other hand, Qu et al. in [29] take advantage of the excellent acoustic properties of AlN and employ an AlN thin-film MEMS acoustic sensor, whose structure is described in [30], to monitor physiological sounds. The authors use a 6-by-7 sensor array to increase the receiving sensitivity and connect 42 circular elements in parallel using Al metal lines. However, the sensor array is covered by Ecoflex 30 silicone polymer since it is fragile and unable to contact human skin directly [29]. Moreover, an air cavity is added to the silicone cover to increase sensitivity and reduce the noise compared to the values obtained using all-silicone packaging before the introduction of the airgap. The proposed sensor was tested for phonocardiogram (PCG) recording by placing it on the chest and validated using ECG signals recorded simultaneously.

In addition to PCG recording, the paper investigates the detection of speech, swallowing, humming, and coughing events by placing the same sensor on the neck. Although the findings are promising, the presented results belong to a single subject under different circumstances. A more detailed and reliable characterization of the device would be achieved by observing multiple subjects of different genders. Furthermore, when placed in direct contact with the skin, the fabricated device is plagued by a low signal-to-noise ratio, forcing the need for a substantially thick silicone polymer package to avoid direct contact with human skin, increasing the overall sensor thickness. The results with all-silicone packaging show a noisy response, which makes air-silicone packaging compulsory for proper measurements.

Dalin et al. presented the physics-based mathematical modeling of an AlN arterial-pulse sensor in [31]. The paper provided numerical simulation results to deliver optimal design parameters for enhanced sensitivity and fatigue stress lifespan. Furthermore, the authors compare radial, carotid, brachial, femoral, and tibial arterial-pulse waveforms of a 25-year-old healthy person with the FEM simulated output voltage of the proposed sensor by inputting the corresponding arterial pulse pressure. Although the paper provides insight into design optimization and performance modeling, it only presents the analytical and simulated results. To understand the functionality and full potential of AlN sensors, experimental results and their validation are essential.

To solve the EMI problem envisioned in [28], Natta et al. proposed an electromagnetic shielding solution reducing the noise induced by capacitive coupling by adding two additional layers to the sensor's heterostructure [32], [33]. Marasco et al. [34] employed the AlN skin sensor introduced by [32], [33] to monitor heart rate by placing the device on the ankle, i.e., above the posterior tibial artery. The work in [34] presents a wearable device communicating in the sub-6GHz 5G ISM band for Internet of Healthcare Things (IoHT) applications. Using the defined communication protocol, the simultaneous monitoring of the pulse waves from the six volunteers comprising females and males between 25 and 29 was achieved. The work described in [34] superficially demonstrates using AlN thin films to monitor heart rate. The paper mainly focuses on the communication protocol and does not characterize the measured signals nor reveal the sensor's full multipurpose capabilities as will be described in this work.

A tabulated summary of the related works discussed is provided in Table 1.While most of the works discussed employ AlN piezoelectric sensors for pulse wave measurement applications from various arteries, only one investigated the acoustic properties of AlN to monitor physiological sounds. In contrast, this work uses the AlN piezoelectric sensor presented in [33] to monitor multiple physiological signals, including heart rhythm, heart sounds, and respiration events. Unlike the sensor in [29], our sensor can be placed directly on the skin thanks to the shielding, allowing us to detect both mechanical deformations and physiological sounds. In addition, we propose a compact, flexible, and biocompatible capsule to protect the ultra-thin sensor structure from damage.

III. METHODOLOGY

This section presents the experimental tools and procedures followed during the realization of this work. The first subsection briefly describes the sensing device used, while the second section describes the hardware setup and data acquisition protocol.

A. SENSING DEVICE

We readopted the AlN-based sensing device described in [33] to monitor multiple physiological signals that can be used to provide CVD risk indices. The sensor is entirely biocompatible and suitable for prolonged use without causing harm to the user. The complete structure of the device is illustrated in Fig. 1, and details of the fabrication process can be found in [28], [32], [33]. The sensor comprises a 1 μm AlN piezoelectric layer sandwiched between Molybdenum (Mo) top and bottom electrodes. The Mo bottom electrode helps achieve high-quality AlN thin films thanks to the low lattice mismatch and the thermal expansion coefficient very close to AlN [35]. The 1 μm AlN piezoelectric layer thickness provides a good compromise between sensor flexibility and piezoelectric properties [28]. In addition, an AlN interlayer is used to improve the crystal orientation of the AlN piezoelectric layer [36], [37]. Also, as mentioned in section II, the sensor has a shielding structure on top to eliminate EMI and capacitive coupling effects [32]. The piezoelectric layer produces an electrical charge in response to mechanical deformations due to blood pulsations or vibrations caused by organ function translated onto the surface of the skin. According to the sensor sensitivity analysis presented in [28], the sensor provides approximately 2 mV in response to a pressure of 5

TABLE 1. Related Works Comparison Table

Parameters	Ref. [27]	Ref. [28]	Ref. [29]	Ref. [31]	Ref. [34]	This Work
Sensor Structure	Pt/Al-AlN-Al	Mo-AlN-Mo	Mo-AlN-Mo	Al-AlN-Al*	Mo-AlN-Mo	Mo-AlN-Mo
Dimensions	-	9.6 mm x 17 mm	2.1 mm x 2.5 mm**	1.5 mm x 1 mm	7.5 mm x 15 mm	7.5 mm x 15 mm
AlN Thickness	1 μm***	1 μm	1 μm	0.5 μm	1 μm	1 μm
EMI Shielding	No	No	No	No	Yes	Yes
Application	Pulse Wave Measurement	Vascular Graft Monitoring	Physiological Sound Monitoring	Pulse Wave Measurement	Pulse Wave Measurement	Multiple Body Signal Monitoring
Experiment Type	In-Vivo	In-Lab	In-Vivo	Simulation	In-Vivo	In-Vivo

* The authors reported that the bottom electrode is composed of a metal layer with a highly-doped silicon layer.
** The reported dimensions are estimated based on a previous publication by the same authors describing a ten-by-ten 3.5 mm x 3.5 mm sensor array.
*** The paper mentions the AlN piezoelectric layer dimension as 1000 μm, which is inconsistent with the total device dimensions reported elsewhere in the same article. Therefore, the unit of μm is assumed to be a typo, and the actual dimension is 1 μm.

kPa. The typical radial blood pressure, according to [31], the typical radial blood pressure is around 5.3 kPa, making the sensor suitable for monitoring radial pulse waves.

The device is skin-conformable due to its ultrathin lightweight profile and flexibility, i.e., it adheres well and conforms to the skin's contours, allowing it to follow skin deformations without causing discomfort. This property allows the sensor to be placed on several body positions, contributing to its versatility. The sensor fabrication procedure allows the shape of the sensor to be easily altered based on the application requirements and body positions. A 3D-printed compact, biocompatible, and flexible capsule was added to the structure described in [33] and illustrated in Fig. 1 to protect the sensor during handling and increase its durability without affecting its conformability. The elastic 50A [38] resin suitable for medical applications manufactured by Formlabs is used to construct the protective capsule. The resin is designed and manufactured using a quality management system certified under ISO 13485 and EU Medical Device Regulation (MDR) standards. The resin is also registered with the USA Food and Drug Administration (FDA) and CE-marked according to the EU MDR, making it safe for medical applications.

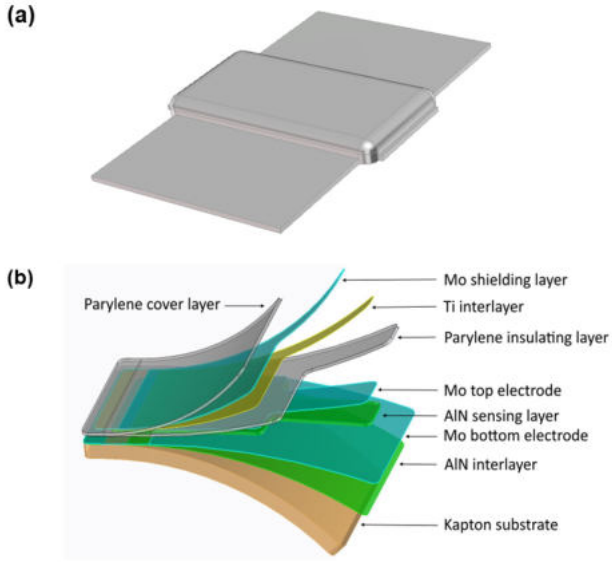

FIGURE 1. Skin sensor overview (a). Biocompatible and flexible capsule with flaps for better skin adhesion (b). AlN piezoelectric sensor multilayer stack

B. EXPERIMENTAL SETUP AND DATA ACQUISITION

We defined an experimental protocol to standardize the data acquisition on the two thirty-year-old healthy volunteer subjects, one male and one female, selected for this study. Information about the experimental setup, protocol, and how their data is processed and stored is given to each volunteer before data collection. After receiving consent, their physiological state, i.e., momentary blood pressure and heart rate, is assessed using a commercial and clinically approved blood pressure monitoring device, OMRON M3 Comfort (HEM-7154-E) [39]. Following this assessment, ECG electrodes are placed according to a 3-electrode ECG system as illustrated in Fig. 2. The Olimex Shield-EKG-EMG open-source hardware board [40] is used to obtain the ECG recordings that serve as reference signals to check the composition, validity, and interpretation accuracy of the signals obtained from the piezoelectric devices. After the correct placement of the ECG electrodes, one or more AlN thin-film piezoelectric skin sensors are placed directly above the desired superficial arteries on the skin surface. The encapsulated sensors are attached to the skin with the help of a commercially available silicone prosthetic adhesive, Derma-Tac [41]. This skin-safe pressure-sensitive adhesive improves the temporary adhesion between the skin surface and the sensor's active area and, therefore, its skin conformability.

The following measurement sites illustrated in Fig. 2 are considered during the initial trials:

- Suprasternal Notch (SSN) for extraction of heart rhythm, heart sounds, and respiration information.
- Collum, i.e., neck, for pulse wave (cardiac rhythm) recordings from the carotid artery.
- Carpus, i.e., wrist, for pulse wave (cardiac rhythm) recordings from the radial artery.

These body positions were particularly selected because they can be located easily, even by non-medically-trained individuals. Additionally, blood pulsations are easily felt over the radial and carotid positions without the need for

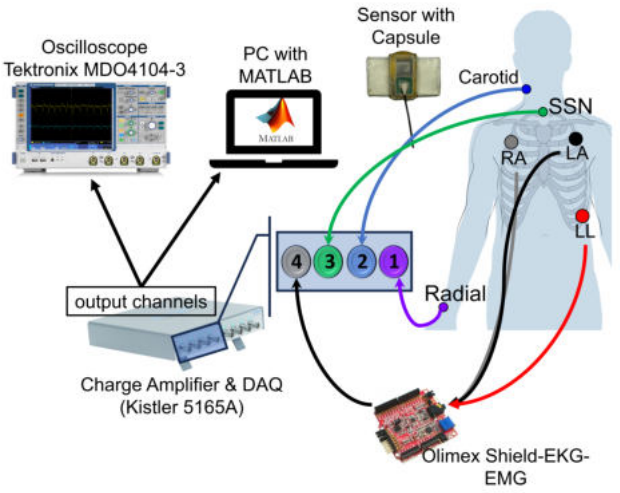

FIGURE 2. Experimental setup; 3-electrode ECG positions RA = Right Arm, LL = Left Arm, LL = Left Leg; Selected pulse wave measurement sites: Collum (Carotid), Carpus (Radial), and Suprasternal Notch

applanation (i.e., the flattening of the artery by applying pressure), as demonstrated by the historical selection of these positions to check one's pulse manually. The SSN is a particular position where we can monitor multiple health parameters. This strategic location permits recording chest movements translated through the SSN, allowing respiration rate extraction. Moreover, the SSN is close to the base of the heart and ascending aorta; therefore, it is also possible to detect blood pulsation and record heart sound components by leveraging the mechano-acoustic properties of the AlN skin sensor [42]. This could help healthcare providers by reducing the time spent on auscultation.

Fig. 2 demonstrates the main instruments used in our experimental setup. The Kistler 5165A [43] 4-channel lab amplifier enables the simultaneous data acquisition of the ECG and piezoelectric signals. The analog output of the ECG device and the AlN sensors are directly connected to the Kistler amplifier. The amplifier has three modes of amplification (charge, voltage, and Integrated Electronics Piezo-Electric (IEPE)), three different filtering options (high-pass, low-pass, and notch filters), and an automatic data acquisition feature. The device is also equipped with a user-control interface that can be used to set the amplification mode, gain, and filters. Similarly, data acquisition settings, such as duration and sampling frequency, can be adjusted from the same interface. Therefore, we take advantage of the voltage amplification, charge amplification, filtering, and data acquisition features of the Kistler to acquire ECG and piezoelectric signals simultaneously. AlN piezoelectric sensor charge output is converted into voltage by using the charge amplifier mode of the Kistler. The gain of the amplifier is set to 10 mV/pC. We also use the second-order high-pass and low-pass filters to filter out very high and low-frequency noise on the output signal. The lab amplifier outputs are also connected to the Tektronix MDO4104-3 oscilloscope [44] to allow signal visualization during acquisition.

Piezoelectric sensor placement combinations were chosen based on the experimental setup configuration, sensor cable lengths, and user comfort. These combinations were used to collect data from the two volunteers over several iterations in one month. Multiple signals were collected during each acquisition session, and only recordings of duration greater than 10s were considered for further analysis. The *carotid - SSN* and *radial - carotid* combinations were observed to be the most suitable placement combinations based on the above-mentioned criteria, with the ECG present as a reference in both instances.

IV. RESULTS AND DISCUSSION

All the acquired data were analyzed using scripts written in MATLAB software. Time and frequency domain correlations among the reference ECG and piezoelectric signals were used to characterize and interpret the observed piezoelectric signals. The ECG signal provides the timing and frequency information for the piezoelectric signal feature characterization and eventual validation of parameters extracted from them. Scalograms of each piezoelectric signal were visually inspected and analyzed to determine the frequency composition of the piezoelectric signals and verify the possible physiological parameters that can be extracted from each pulse wave. The following subsections discuss the results obtained from our initial trials and outline the signal feature characterization procedures followed. As mentioned in section III, two sensor placement combinations were used during data collection; however, for conciseness, only the carotid signal from the *radial-carotid* signal is considered in this section.

A. SIGNAL MORPHOLOGY AND COMPOSITION

Fig. 3 illustrates the typical shapes and time domain characteristics of the pulse wave signals obtained from the selected sensor positions on each volunteer. The dominant time-frequency characteristics remain constant among the signals from all the selected positions due to the nature of the events that translate into the skin deformations and prompt the piezoelectric response. From this pattern, we can deduce that the main systolic event can be gathered from any selected position. The deformation due to the systolic upstroke, i.e., the largest pressure change during a heart cycle as depicted in Fig. 10, translates to the most prominent visible peaks within the recorded pulse waves. The definition of the other events, such as the ventricular diastole, are also translated into deformations of lower amplitudes; however, several factors, including sensor position, determine their definition and clarity. More detailed information about the components of each signal can be extracted by performing a frequency domain analysis of each signal. Fig. 4 shows the frequency components of the signals from each selected position, revealing the subtle variations observed between signals obtained from the two volunteers. As the scalograms

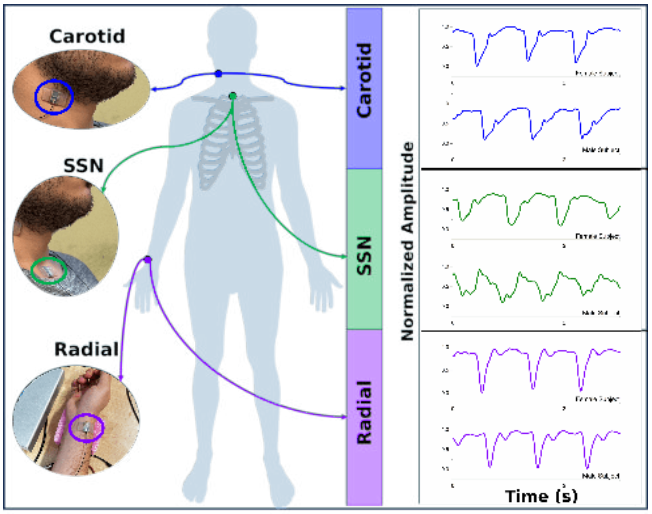

FIGURE 3. Carotid, SSN, and Radial pulse wave signal time domain characteristics. *NB: Amplitudes are unitless and normalized between 0 and 1*

demonstrate, several periodic patterns are embedded within the measured pulse waves. The dominant frequency in all the observed signals is around 1 Hz, illustrating the possibility of extracting heart rate information, typically between 1 and 1.67 Hz in healthy adults, from all signals [45]. The carotid and SSN signals also reveal frequencies below 0.5 Hz, corresponding to the breathing rate (BR), which in resting healthy adults can lie between 0.2 and 0.3 Hz [46]. Comparing the ECG signal time-frequency scalograms in Fig. 5 to the piezoelectric scalograms in Fig. 4, periodic frequency components between 5 Hz and 50 Hz are distinguishable in both cases. For instance, in the ECG scalogram, the dominant frequency within this range corresponds to the QRS complex, depicting ventricular depolarization. This observation shows that the piezoelectric pulse waves can be used to delineate various stages of the heart cycle, which are helpful for extracting more complex CVD indices. The definition of similar components in the pulse waves varies with the measurement site; therefore, the heart cycle delineation can be performed with varying degrees of accuracy. As a result, the choice of measurement site can affect the required signal processing and event delineation accuracy.

B. PULSE RATE

All the selected sensor positions provide pulse rate information. Therefore, if the desired application only requires heart rate information, the sensor position can be chosen based on user comfort and preference. The most prominent signal peaks corresponding to the largest deformation detected were used to determine the heart rate from each pulse wave signal. The Python-based neurophysiological signal processing toolbox Neurokit2 (NK) [47] heart rate estimation functions were integrated with MATLAB and applied to the signal peaks. The same algorithm was also used to estimate the heart rate from the reference ECG signal after R peak detection. Sev-

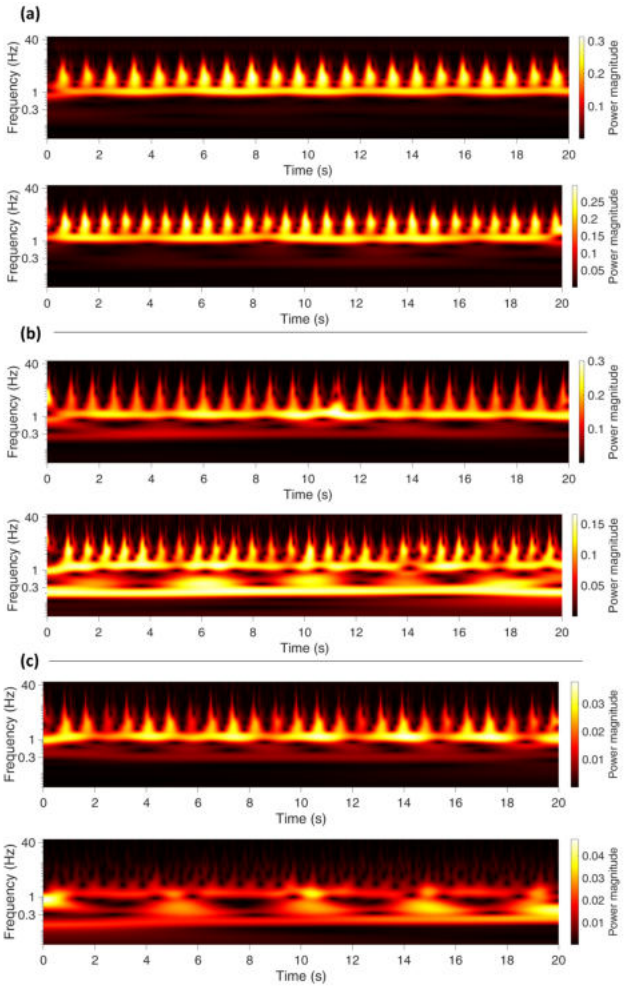

FIGURE 4. Pulse wave signal Time Frequency Scalograms from male and female volunteers. Scalograms obtained from 20s-long signal snippets. (a) radial (top female, bottom male), (b) carotid (top female, bottom male), (c) Suprasternal Notch (top female, bottom male). *NB: Amplitudes are unitless and normalized between 0 and 1*

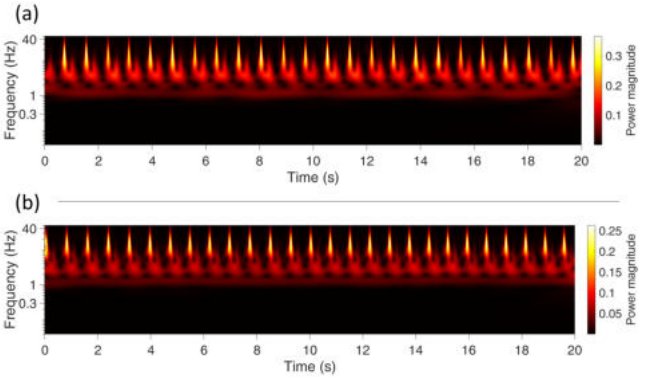

FIGURE 5. ECG signal scalograms obtained from 20s-long snippets. (a)scalogram corresponding to the ECG signal from the female volunteer (b)scalogram corresponding to the ECG signals from the male volunteer. Both ECG signals were simultaneously recorded with the SSN signal illustrated in Fig. 4(c) *NB: Amplitudes are unitless and normalized between 0 and 1*

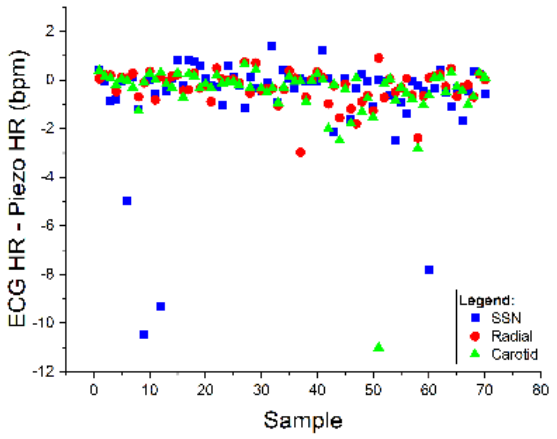

FIGURE 6. Pulse Wave signal HR estimation differences in beats per minute (bpm) for each 10-second sample compared to corresponding ECG reference signal

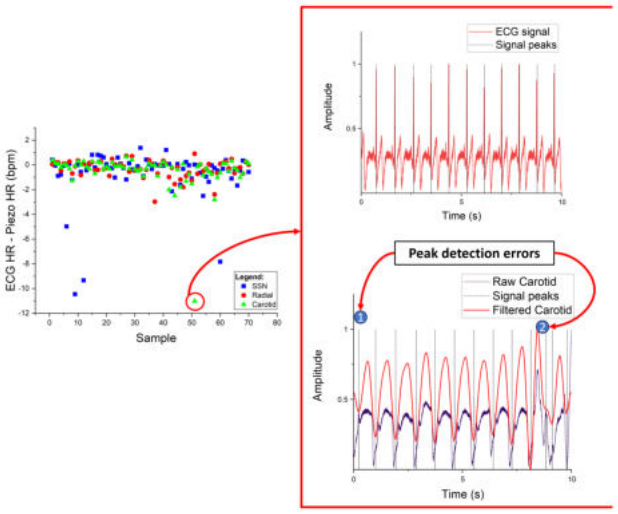

FIGURE 7. Heart rate estimation outlier pulse wave example. BPM estimation error attributed to the extra peaks labeled 1 & 2. *NB: Amplitudes are unitless and normalized between 0 and 1*

enty 10s-long signal segments were selected from the signals collected from the two volunteers at each measurement site, and the HR was estimated for each sample. Fig. 6 illustrates the bpm difference between the ECG HR estimation and the values obtained from the different pulse wave signals. A few outliers corresponding to low-quality pulse wave signals like the one illustrated in Fig. 7 are observed in Fig. 6. In this case, outliers are values greater than two standard deviations from the regression line. The sample corresponding to one of the outliers is illustrated in Fig. 7. Two extra peaks (labeled 1 and 2) can be observed in the pulse wave signal. Therefore, employing signal quality assessment and more rigorous peak detection algorithms based on advanced signal morphology, pattern detection, or artificial intelligence methods can increase the pulse wave signal HR estimation accuracy. This conclusion is corroborated by Fig. 8 illustrating improved estimation accuracy after removing outliers. The resulting maximum deviation observed after removing outliers is below the widely accepted 5 bpm maximum error [48]. Additionally, strong linear correlations exist between the piezoelectric HR estimation results and corresponding reference ECG estimations. The r values of 0.81 for the SSN and 0,99 for both the radial and carotid estimations validate this claim. We can conclude that the radial and carotid positions provide more accurate pulse rate information when compared to the SSN-derived pulse rate.

C. BREATHING RATE

In addition to the heart rate signal, a periodic pattern around 0.3 Hz is observed in the time-frequency scalogram plots shown in Fig. 4, corresponding to the breathing rate, which typically falls between 0.2 and 0.33 Hz [46], i.e., between 12 and 20 breaths per minute. Therefore, pulse wave signals from the carotid and SSN positions can be used to obtain respiration signals accurately. During data acquisition, each

FIGURE 8. Effect of low-quality signal samples on HR estimation. Top: deviation from ECG reference when low-quality signals are included; Bottom: deviation from ECG reference when low-quality signals are excluded

volunteer was asked to breathe normally while their chest movements were manually observed to capture the number of breaths taken. Two 100s long recordings were obtained from each volunteer to perform preliminary conclusions. The pulse wave signals are filtered using a 0.15-0.35 Hz band pass filter to confirm the number of breaths determined by the manual observations. Fig. 9 shows excerpts of the carotid and SSN pulse waves used to verify respiration signal extraction. The number of breaths manually observed during data acquisition agrees, with a maximum deviation of one breath, with the values extracted from the recorded signals as detailed in Table 2. Therefore, the respiration signal can be extracted by applying the appropriate low-frequency bandpass filters to eliminate other signal components from the carotid and SSN pulse waves. Consequently, using existing algorithms,

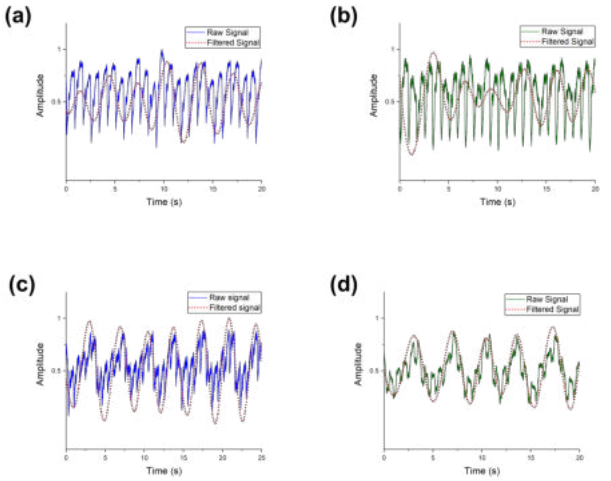

FIGURE 9. 20s excerpts of raw signals and bandpass filtered signals (a). Female Subject carotid (b). Female Subject SSN (c). Male Subject carotid (d). Male Subject SSN. *NB: Amplitudes are unitless and normalized between 0 and 1*

TABLE 2. Number of breaths: manual observation Vs. extracted from 100s-long SSN and carotid pulse waves

	Female Subject			Male subject		
Sample number	Manual	SSN	Carotid	Manual	SSN	Carotid
1	32	31	31	28	27	27
2	31	30	31	30	30	30

the respiration signal can be used to estimate the breathing rate. The four 100-second signals, two samples from each volunteer, were given as inputs to the NK toolbox respiration rate estimation algorithm, resulting in values between ≈16.34 and 19 breaths per minute. The estimated values fall within the range expected for healthy adults.

D. HEART SOUNDS

Heart sounds produced by heart valve movements and blood flow through the vessels are useful for diagnosing CVDs [49]–[51]. The normal audible heart sounds typically follow a periodic pattern of 2 pulses, the first and second heart sounds, (S1) and (S2) Fig. 10, with frequencies between 20 and 150 Hz [7], [50]. Since the AlN films can detect the physical vibrations produced by the mechanical events of the heart muscles of the sounds [42], we hypothesize that the signal obtained from the SSN measurement site, situated closest to the heart, contains the S1 and S2 heart sound components. The sensor deforms in response to the mechanical vibrations translated from the heart onto the chest wall, allowing us to obtain a signal containing information corresponding to the valve closures, i.e., S1 and S2. The time-frequency scalograms in 4 (c) show barely visible, low-power magnitude, short-burst periodic signal components above 10 Hz, partially corroborating our hypothesis. Therefore, after removing the lower-frequency components, S1 and S2 can be clearly distinguished, as shown in the time-frequency scalograms in Fig. 11. Fig. 11 also illustrates the relationship between the S1 and S2 component locations and ECG signal events, a result in agreement with the PCG and ECG relationship demonstrated in the wiggers diagram in Fig. 10.

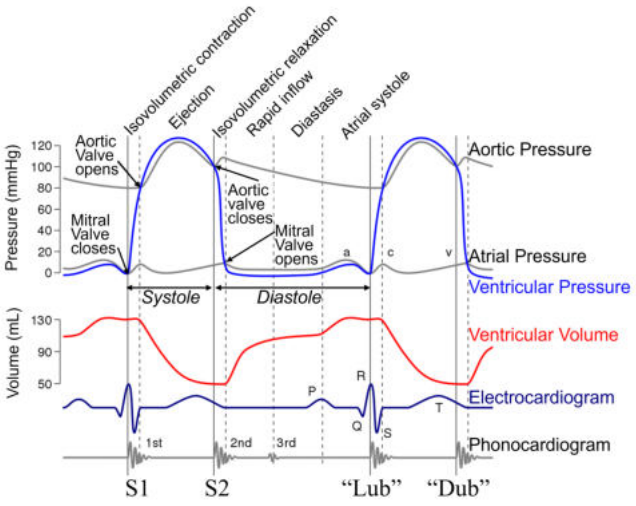

FIGURE 10. Wiggers diagram of the left side of the heart showing phases of the electrocardiogram (ECG), phonocardiogram (PCG), and pressure changes that occur during a heart cycle. Image adapted from [52]

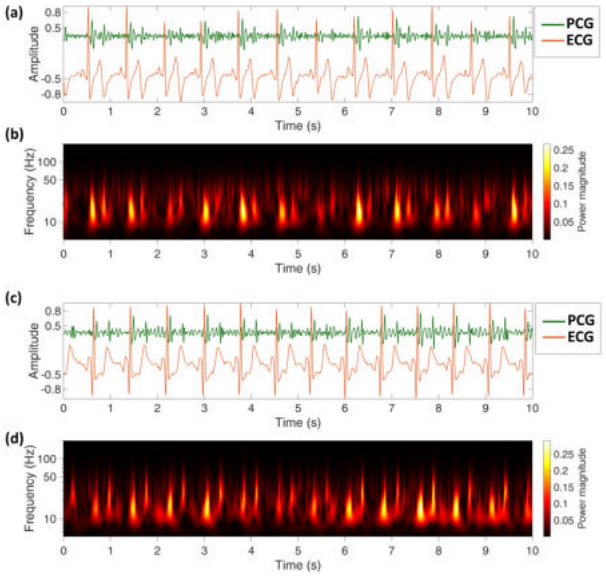

FIGURE 11. (a). Female SSN-extracted PCG signal and corresponding ECG (b). Female PCG time-frequency scalogram (c). Male SSN-extracted PCG signal and corresponding ECG (d). Male PCG time-frequency scalogram *NB: Amplitudes are unitless and normalized between 0 and 1*

V. CONCLUSION AND FUTURE PERSPECTIVES

We have successfully demonstrated the feasibility of using AlN thin films to develop a bio-compatible device that can be used to monitor multiple physiological signals that can facilitate the evaluation of several CVD risk indices. We characterized the morphology of the signals measured from the radial, carotid, and SSN positions and verified the ex-

tracted physiological parameters using reference ECG signals, widely used in clinical practice, and manually observed physiological phenomenon demonstrating the viability of our device. Our observations show that measurement sites can be selected according to the required information. The signal collected from the SSN provides all the parameters characterized in this paper, i.e., BR, HR, and heart sounds; however, based on the executed MATLAB scripts, heart sound extraction required more signal processing steps, translating to higher computational and temporal costs. The observed error between the pulse rate extracted from the piezoelectric pulse waves obtained from all observed positions and the ECG reference is within acceptable margins. The SSN provides less accurate pulse rate information. Therefore, we can conclude that obtaining multiple signals from the SSN requires a trade-off in the pulse rate accuracy.

In addition to its bio- and CMOS-compatibility, the AlN piezoelectric skin sensors demonstrate encouraging performance in providing signals embedding multiple physiological parameters, which can provide crucial cardiodynamic parameters. Further experiments are required to provide a rigorous performance evaluation of our sensor on a larger and more diverse sample size; therefore, our next steps include verifying the test results in a clinical environment. Based on the feedback from the clinical trials, we intend to improve the capsule design to optimize comfort and enhance the versatility of our device. Moreover, integrating the device with comfortable fabrics and a small footprint PCB is one of our envisioned future steps towards developing a wireless smart textile product that can continuously extract the desired CVD-related parameters.

The fabricated devices exhibit mechano-acoustic behavior, hence the heart sound detection, and are currently being analyzed for other applications, including speech recognition applications. The sensor is also being tested for respiratory sound recording to perform auscultation and decrease the workload of healthcare providers. The same sensor has also been tested before for detecting swallowing disorders and sleep monitoring from eye movements. One of the key challenges we aim to address is the use of a minimum number of sensors with small-footprint electronics to detect the maximum number of vital parameters simultaneously. Therefore, this device demonstrates a versatile and multipurpose healthcare asset to augment healthcare professionals by providing multiple high-quality physiological parameters. Additionally, the data collected using our experiments are also currently being organized to create datasets for relevant applications for the benefit of the scientific community. The use of AI algorithms to develop complete smart environments for remote diagnosis and therapeutics is also envisioned. Therefore, our work exhibits a multidisciplinary contribution to various Internet of Medical Things (IoMT) enabling sectors.

REFERENCES

[1] M. A. Scrugli, D. Loi, L. Raffo, and P. Meloni, "An adaptive cognitive sensor node for ecg monitoring in the internet of medical things," IEEE Access, vol. 10, pp. 1688–1705, 2022.

[2] J.-W. Chen, H.-K. Huang, Y.-T. Fang, Y.-T. Lin, S.-Z. Li, B.-W. Chen, Y.-C. Lo, P.-C. Chen, C.-F. Wang, and Y.-Y. Chen, "A data-driven model with feedback calibration embedded blood pressure estimator using reflective photoplethysmography," Sensors, vol. 22, no. 5, 2022.

[3] WHO, "Cardiovascular diseases," https://www.who.int/news-room/fact-sheets/detail/cardiovascular-diseases-(cvds), acessed: 10 July 2023.

[4] G. V. Ramani, P. A. Uber, and M. R. Mehra, "Chronic heart failure: Contemporary diagnosis and management," Mayo Clinic Proceedings, vol. 85, no. 2, pp. 180–195, 2010.

[5] R. Bouhenguel and I. Mahgoub, "A risk and incidence based atrial fibrillation detection scheme for wearable healthcare computing devices," in 2012 6th International Conference on Pervasive Computing Technologies for Healthcare (PervasiveHealth) and Workshops, May 2012, pp. 97–104.

[6] C. Liu, D. Springer, Q. Li, B. Moody, R. A. Juan, F. J. Chorro, F. Castells, J. M. Roig, I. Silva, A. E. W. Johnson, Z. Syed, S. E. Schmidt, C. D. Papadaniil, L. Hadjileontiadis, H. Naseri, A. Moukadem, A. Dieterlen, C. Brandt, H. Tang, M. Samieinasab, M. R. Samieinasab, R. Sameni, R. G. Mark, and G. D. Clifford, "An open access database for the evaluation of heart sound algorithms," Physiol Meas, vol. 37, no. 12, pp. 2181–2213, Dec 2016.

[7] S. N. Ali, S. B. Shuvo, M. I. S. Al-Manzo, A. Hasan, and T. Hasan, "An end-to-end deep learning framework for real-time denoising of heart sounds for cardiac disease detection in unseen noise," IEEE Access, vol. 11, pp. 87 887–87 901, 2023.

[8] D. Zhang, X. Liu, J. Xia, Z. Gao, H. Zhang, and V. H. C. de Albuquerque, "A physics-guided deep learning approach for functional assessment of cardiovascular disease in iot-based smart health," IEEE Internet of Things Journal, vol. 10, no. 21, pp. 18 505–18 516, 2023.

[9] J. Mant, J. Doust, A. Roalfe, P. Barton, M. R. Cowie, P. Glasziou, D. Mant, R. J. McManus, R. Holder, J. Deeks, K. Fletcher, M. Qume, S. Sohanpal, S. Sanders, and F. D. R. Hobbs, "Systematic review and individual patient data meta-analysis of diagnosis of heart failure, with modelling of implications of different diagnostic strategies in primary care," Health Technol. Assess., vol. 13, no. 32, pp. 1–207, iii, Jul 2009.

[10] J. Knuuti, W. Wijns, A. Saraste, D. Capodanno, E. Barbato, C. Funck-Brentano, E. Prescott, R. F. Storey, C. Deaton, T. Cuisset, S. Agewall, K. Dickstein, T. Edvardsen, J. Escaned, B. J. Gersh, P. Svitil, M. Gilard, D. Hasdai, R. Hatala, F. Mahfoud, J. Masip, C. Muneretto, M. Valgimigli, S. Achenbach, J. J. Bax, and ESC Scientific Document Group, "2019 ESC guidelines for the diagnosis and management of chronic coronary syndromes," Eur. Heart J., vol. 41, no. 3, pp. 407–477, Jan 2020.

[11] G. Hindricks, T. Potpara, N. Dagres, E. Arbelo, J. J. Bax, C. Blomström-Lundqvist, G. Boriani, M. Castella, G.-A. Dan, P. E. Dilaveris, L. Fauchier, G. Filippatos, J. M. Kalman, M. La Meir, D. A. Lane, J.-P. Lebeau, M. Lettino, G. Y. H. Lip, F. J. Pinto, G. N. Thomas, M. Valgimigli, I. C. Van Gelder, B. P. Van Putte, C. L. Watkins, and ESC Scientific Document Group, "2020 ESC guidelines for the diagnosis and management of atrial fibrillation developed in collaboration with the european association for Cardio-Thoracic surgery (EACTS): The task force for the diagnosis and management of atrial fibrillation of the european society of cardiology (ESC) developed with the special contribution of the european heart rhythm association (EHRA) of the ESC," Eur. Heart J., vol. 42, no. 5, pp. 373–498, Feb 2021.

[12] B. Williams, G. Mancia, W. Spiering, E. Agabiti Rosei, M. Azizi, M. Burnier, D. L. Clement, A. Coca, G. de Simone, A. Dominiczak, T. Kahan, F. Mahfoud, J. Redon, L. Ruilope, A. Zanchetti, M. Kerins, S. E. Kjeldsen, R. Kreutz, S. Laurent, G. Y. H. Lip, R. McManus, K. Narkiewicz, F. Ruschitzka, R. E. Schmieder, E. Shlyakhto, C. Tsioufis, V. Aboyans, I. Desormais, and ESC Scientific Document Group, "2018 ESC/ESH guidelines for the management of arterial hypertension," Eur. Heart J., vol. 39, no. 33, pp. 3021–3104, Sep 2018.

[13] M. Galderisi, B. Cosyns, T. Edvardsen, N. Cardim, V. Delgado, G. Di Salvo, E. Donal, L. E. Sade, L. Ernande, M. Garbi, J. Grapsa, A. Hagendorff, O. Kamp, J. Magne, C. Santoro, A. Stefanidis, P. Lancellotti, B. Popescu, G. Habib, 2016-2018 EACVI Scientific Documents Committee, and 2016-2018 EACVI Scientific Documents Committee, "Standardization of adult transthoracic echocardiography reporting in agreement with recent chamber quantification, diastolic function, and heart valve disease recommendations: an expert consensus document of the

european association of cardiovascular imaging," Eur. Heart J. Cardiovasc. Imaging, vol. 18, no. 12, pp. 1301–1310, Dec 2017.

[14] J. Lin, R. Fu, X. Zhong, P. Yu, G. Tan, W. Li, H. Zhang, Y. Li, L. Zhou, and C. Ning, "Wearable sensors and devices for real-time cardiovascular disease monitoring," Cell Reports Physical Science, vol. 2, no. 8, p. 100541, Aug 2021.

[15] A. Bhattarai, D. Peng, J. Payne, and H. Sharif, "Adaptive partition of ECG diagnosis between cloud and wearable sensor net using open-loop and closed-loop switch mode," IEEE Access, vol. 10, pp. 63 684–63 697, 2022.

[16] J. Émile S. Kenny, I. Barjaktarevic, A. M. Eibl, M. Parrotta, B. F. Long, and J. K. Eibl, "The feasibility of a novel, wearable doppler ultrasound to track stroke volume change in a healthy adult," Journal of Emergency and Critical Care Medicine, vol. 4, Apr 2020.

[17] L. Li, L. Zhao, R. Hassan, and H. Ren, "Review on wearable system for positioning ultrasound scanner," Machines, vol. 11, no. 3, p. 325, Feb 2023.

[18] G. Chen, C. Au, and J. Chen, "Textile triboelectric nanogenerators for wearable pulse wave monitoring," Trends in Biotechnology, vol. 39, no. 10, pp. 1078–1092, Oct 2021.

[19] K. Meng, X. Xiao, W. Wei, G. Chen, A. Nashalian, S. Shen, X. Xiao, and J. Chen, "Wearable pressure sensors for pulse wave monitoring," Advanced Materials, vol. 34, no. 21, p. 2109357, Mar 2022.

[20] Y. Chu, J. Zhong, H. Liu, Y. Ma, N. Liu, Y. Song, J. Liang, Z. Shao, Y. Sun, Y. Dong, X. Wang, and L. Lin, "Human pulse diagnosis for medical assessments using a wearable piezoelectret sensing system," Advanced Functional Materials, vol. 28, no. 40, p. 1803413, 2018.

[21] S. Marauska, T. Dankwort, H. Quenzer, and B. Wagner, "Sputtered thin film piezoelectric aluminium nitride as a functional MEMS material and CMOS compatible process integration," Procedia Engineering, vol. 25, pp. 1341–1344, 2011.

[22] M. Zhang, J. Yang, C. Si, G. Han, Y. Zhao, and J. Ning, "Research on the piezoelectric properties of AlN thin films for MEMS applications," Micromachines, vol. 6, no. 9, pp. 1236–1248, Sep 2015.

[23] M. Mariello, F. Guido, L. Algieri, V. M. Mastronardi, A. Qualtieri, F. Pisanello, and M. De Vittorio, "Microstructure and electrical properties of novel piezo-optrodes based on thin-film piezoelectric aluminium nitride for sensing," IEEE Transactions on Nanotechnology, vol. 20, pp. 10–19, 2021.

[24] W. R. Ali and M. Prasad, "Piezoelectric MEMS based acoustic sensors: A review," Sensors and Actuators A: Physical, vol. 301, p. 111756, Jan 2020.

[25] R. S. Fazzio, T. Lamers, O. Buccafusca, A. Goel, and W. Dauksher, "Design and performance of aluminum nitride piezoelectric microphones," in TRANSDUCERS 2007 - 2007 International Solid-State Sensors, Actuators and Microsystems Conference. IEEE, 2007, pp. 1255–1258.

[26] S. T. Haider, M. A. Shah, D.-G. Lee, and S. Hur, "A review of the recent applications of aluminum nitride-based piezoelectric devices," IEEE Access, vol. 11, pp. 58 779–58 795, 2023.

[27] A. Bongrain, L. Rousseau, L. Valbin, N. Madaoui, G. Lissorgues, F. Verjus, and P. A. Chapon, "A new technology of ultrathin AlN piezoelectric sensor for pulse wave measurement," Procedia Eng., vol. 120, pp. 459–463, 2015, Eurosensors 2015.

[28] L. Natta, V. M. Mastronardi, F. Guido, L. Algieri, S. Puce, F. Pisano, F. Rizzi, R. Pulli, A. Qualtieri, and M. De Vittorio, "Soft and flexible piezoelectric smart patch for vascular graft monitoring based on aluminum nitride thin film," Scientific Reports, vol. 9, p. 8392, Jun. 2019.

[29] M. Qu, X. Chen, D. Yang, D. Li, K. Zhu, X. Guo, and J. Xie, "Monitoring of physiological sounds with wearable device based on piezoelectric MEMS acoustic sensor," Journal of Micromechanics and Microengineering, vol. 32, no. 1, p. 014001, Nov 2021.

[30] X. Chen, C. Liu, D. Yang, X. Liu, L. Hu, and J. Xie, "Highly accurate airflow volumetric flowmeters via pMUTs arrays based on transit time," Journal of Microelectromechanical Systems, vol. 28, no. 4, pp. 707–716, 2019.

[31] E. M. Dalin and S. M. R. Hasan, "Modeling of a novel AlN nanogenerator-based self-powered MEMS arterial-pulse sensor," IEEE Sensors Journal, vol. 22, no. 9, pp. 8574–8582, 2022.

[32] L. Natta, P. Lombardi, V. Mastronardi, F. Guido, A. Qualtieri, M. Di Rienzo, and M. De Vittorio, "Flexible piezoelectric sensor with integrated electromagnetic shield," Dec 2022, US Patent App. 17/780,221.

[33] L. Natta, F. Guido, L. Algieri, V. M. Mastronardi, F. Rizzi, E. Scarpa, A. Qualtieri, M. T. Todaro, V. Sallustio, and M. D. Vittorio, "Conformable AlN piezoelectric sensors as a non-invasive approach for swallowing disorder assessment," ACS Sensors, vol. 6, pp. 1761–1769, May 2021.

[34] I. Marasco, G. Niro, S. M. Demir, L. Marzano, L. Fachechi, F. Rizzi, D. Demarchi, P. Motto Ros, A. D'Orazio, M. Grande, and M. De Vittorio, "Wearable heart rate monitoring device communicating in 5G ISM band for IoHT," Bioengineering, vol. 10, no. 1, 2023.

[35] J.-B. Lee, J.-P. Jung, M.-H. Lee, and J.-S. Park, "Effects of bottom electrodes on the orientation of AlN films and the frequency responses of resonators in AlN-based FBARs," Thin Solid Films, vol. 447-448, pp. 610–614, Jan 2004, Proceedings of the 30th International Conference on Metallurgical Coatings and Thin Films.

[36] T. Kamohara, M. Akiyama, and N. Kuwano, "Influence of molybdenum bottom electrodes on crystal growth of aluminum nitride thin films," Journal of Crystal Growth, vol. 310, no. 2, pp. 345–350, 2008.

[37] H. Matsumoto, K. Asai, N. Kobayashi, S. Nagashima, A. Isobe, N. Shibagaki, and M. Hikita, "Influence of underlayer materials on preferred orientations of sputter-deposited AlN/mo bilayers for film bulk acoustic wave resonators," Japanese Journal of Applied Physics, vol. 43, no. 12R, pp. 8219–8222, Dec 2004.

[38] Formlabs, "3D printing materials for healthcare," https://formlabs.com/materials/medical/, accessed: 7 August 2023.

[39] O. healthcare, "Omron M3 comfort blood pressure monitor," https://www.omron-healthcare.com/eu/blood-pressure-monitors/m3_comfort_2.html, accessed: 7 August 2023.

[40] Olimex, "SHIELD-EKG-EMG - open source hardware board," https://www.olimex.com/Products/Duino/Shields/SHIELD-EKG-EMG/open-source-hardware, accessed: 7 August 2023.

[41] I. Smooth-On, "Derma-tac product information," https://www.smooth-on.com/products/derma-tac/, accessed: 8 August 2023.

[42] S. M. Demir, L. Marzano, P. Motto Ros, L. Fachechi, D. Demarchi, and M. De Vittorio, "Wearable multiple body signal monitoring system with single biocompatible AlN piezoelectric sensor," in 2023 IEEE International Symposium on Circuits and Systems (ISCAS), 2023, pp. 1–5.

[43] K. Group, "Laboratory charge amplifiers labamp with data acquisition, for dynamic and or quasi-static signals, up to 8 channels," https://www.kistler.com/IT/en/cp/laboratory-charge-amplifiers-labamp-with-data-acquisition-labamp/P0000289, accessed: 7 August 2023.

[44] I. Tektronix, "Mixed domain oscilloscopes," https://www.tek.com/en/datasheet/mixed-domain-oscilloscopes-0, accessed: 7 August 2023.

[45] Z. Yi, W. Zhang, and B. Yang, "Piezoelectric approaches for wearable continuous blood pressure monitoring: A review," Journal of Micromechanics and Microengineering, vol. 32, no. 10, p. 103003, Aug 2022.

[46] X. Bao, A. K. Abdala, and E. N. Kamavuako, "Estimation of the respiratory rate from localised ECG at different auscultation sites," Sensors, vol. 21, no. 1, p. 78, Dec 2020.

[47] D. Makowski, T. Pham, Z. J. Lau, J. C. Brammer, F. Lespinasse, H. Pham, C. Schölzel, and S. H. A. Chen, "NeuroKit2: A python toolbox for neurophysiological signal processing," Behavior Research Methods, vol. 53, no. 4, pp. 1689–1696, Feb 2021.

[48] M. Hassan, A. Malik, D. Fofi, B. Karasfi, and F. Meriaudeau, "Towards health monitoring using remote heart rate measurement using digital camera: A feasibility study," Measurement, vol. 149, p. 106804, Jan 2020.

[49] R. Nersisson and M. M. Noel, "Heart sound and lung sound separation algorithms: A review," Journal of Medical Engineering & Technology, vol. 41, no. 1, pp. 13–21, Jul 2016.

[50] F. Arvin, S. Doraisamy, and E. Safar Khorasani, "Frequency shifting approach towards textual transcription of heartbeat sounds," Biological Procedures Online, vol. 13, no. 1, p. 7, Oct 2011.

[51] K. Phua, J. Chen, T. H. Dat, and L. Shue, "Heart sound as a biometric," Pattern Recognition, vol. 41, no. 3, pp. 906–919, Mar 2008.

[52] G. Medics, "The cardiac cycle: Wigger's diagram," https://geekymedics.com/the-cardiac-cycle/, May 2022, acessed: 3 August 2023.

ANGELA TAFADZWA SHUMBA (Graduate Student Member, IEEE) received the M. Eng. degree in Electrical Engineering from the Cape Peninsula University of Technology, Cape Town, (South Africa), and completed an M.Sc. degree in Electric and Electronic Systems Engineering from Ecole Supérieure d'Ingénieurs en Electronique et Electrotechnique (ESIEE), Paris, (France) through the French South African Institute of Technology (F'SATI) in 2018. Her master's thesis, "Channel Coding on a Nanosatellite Platform," involved developing FPGA implementations of a 1⁄2-rate convolutional encoder and the corresponding Viterbi decoder for CubeSat communications. She is working towards a Ph.D. in complex systems engineering at the University of Salento, Italy. She is affiliated with the Centre for Biomolecular Nanotechnologies (CBN), Istituto Italiano di Tecnologia (IIT), and the IDentification Automation (IDA) Laboratory, Lecce (Italy). Her research interests include Embedded Systems, data processing and analysis technologies, and IoT infrastructures based on novel sensing technologies, such as biocompatible piezoelectric transducers, towards developing reliable smart environments for various applications, especially healthcare.

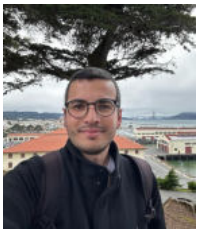

SULEYMAN MAHIRCAN DEMIR (Graduate Student Member, IEEE) received the B.S. and M.S. in electrical and electronics engineering from Middle East Technical University (METU), Northern Cyprus Campus (NCC) in 2017 and 2020, respectively. He is currently pursuing a Ph.D. degree in electronics engineering at Politecnico di Torino and conducting his research activities at Istituto Italiano di Tecnologia (IIT), Center for Biomolecular Nanotechnologies (CBN). His research interests include integrated circuit design, energy harvesting, low-power electronics, interface circuit design for MEMS sensors, and wearable devices for health monitoring.

VINCENZO MARIANO MASTRONARDI received the M.S. degree in Ingegneria delle Telecomunicazioni in 2012 at the Università del Salento, Lecce (Italy). In 2016, he earned his Ph.D. in Material Science and Technology at the Center for Biomolecular Nanotechnologies (IIT), Lecce (Italy), and received the degree of highly qualified Research Doctor in Nanotechnologies and Nanostructured Innovative Materials from Scuola Interpolitecnica di Dottorato (SIPD), Torino (Italy). From 2016 to 2021, he was a post-doc at the Center for Biomolecular Nanotechnologies (IIT), Lecce (Italy). Since 2022, he has been a researcher at the Department of Innovation Engineering of Università del Salento, Lecce (Italy). His research interests include wearable and inertial sensors, flexible and silicon-based MEMS, and piezoelectric energy harvester devices.

FRANCESCO RIZZI received the Ph.D. degree in physics, in 2004. He is a Research Staff Member with the Center of Biomolecular Nanotechnologies, Istituto Italiano di Tecnologia, Lecce. He held postdoctoral training with the Department of Physics, Institute of Photonics, University of Strathclyde, Glasgow, U.K., where he won an Experienced Researcher Marie Curie Fellowship. He has authored more than 70 manuscripts in international journals and proceedings of international conferences, two patents, and three book chapters. His research interests and activities are related to bioinspired microelectromechanical systems design and fabrication for applications in biological and environmental sensing and artificial hair cell fabrication for flow sensing in robotics.

GAIA DE MARZO received her M.S. degree in Nanobiotechnology at the University of Trieste in 2018. In 2022, she received her PhD in Materials and Structures Engineering and Nanotechnology at the University of Salento and Center for Biomolecular Nanotechnologies (CBN), Istituto Italiano di Tecnologia (IIT), Lecce (Italy). She is currently enrolled as a PostDoc fellow at CBN-IIT. Her research focuses on flexible and wearable devices based on piezoelectric biopolymers for drug delivery, sensing physiological strains, and ultrasound."

LUCA FACHECHI is a researcher at the Center for Biomolecular Nanotechnologies (CBN) of the Istituto Italiano di Tecnologia (IIT). His research focuses on sensors powered by vibrational harvested energy using piezoelectric and triboelectric transducers and developing electronic front-end solutions for sensors. He has long research and industry expertise in electronic hardware design, firmware implementation, and wireless sensor networks.

PAOLO MOTTO ROS (Member, IEEE) received the M.Sc. and Ph.D. degrees in electronic engineering from the Politecnico di Torino, Italy, in 2005 and 2009, respectively. Assistant Professor at Politecnico di Torino, Department of Electronics and Telecommunications, Turin, Italy. Post-doc researcher at Politecnico di Torino (2009–2012), senior (since 2014) post-doc researcher at Istituto Italiano di Tecnologia (2012–2019), senior post-doc researcher and adjunct professor (since 2017) at Politecnico di Torino (2019–2022). Author and co-author of more than 80 international scientific publications. Dr. Motto Ros was a member of the organizing committee of IEEE ICECS 2019, the FoodCAS Satellite Event at IEEE ISCAS 2021 and IEEE CAFE 2023, review committee member of IEEE BioCAS 2021 and 2022, special session organizer at IEEE MeMeA 2021, program committee member of IEEE LASCAS 2022, guest editor of MDPI Sensors and guest associate editor of Frontiers in Neurorobotics; he is Associate Editor of IEEE Transactions on AgriFood Electronics and IEEE Transactions on Biomedical Circuits and Systems.

DANILO DEMARCHI (Senior Member, IEEE) received Engineering Degree and Ph.D. in electronics engineering from Politecnico di Torino, Italy, in 1991 and 1995, respectively. Full Professor at Politecnico di Torino, Department of Electronics and Telecommunications, Turin, Italy. Visiting Professor at Tel Aviv University (2018-2021) and at EPFL Lausanne (2019). Visiting Scientist at MIT and Harvard Medical School (2018). Author and co-author of 5 patents and more than 300 international scientific publications. Prof. Demarchi is the leader of the MiNES (MicroNano Electronic Systems) Laboratory at Politecnico di Torino, Member of IEEE Sensors Council, Member of the IEEE BioCAS Technical Committee, Associate Editor of IEEE Sensors Journal, of the IEEE Open Journal of Engineering in Medicine and Biology and of the Springer Journal BioNanoScience, General Chair of IEEE BioCAS 2017 and founder of the IEEE FoodCAS

LUIGI PATRONO (Member, IEEE) received the M.S. degree in computer engineering from the University of Lecce, Italy, in 1999, and the Ph.D. degree in innovative materials and technologies for satellite networks from the ISUFI-University of Lecce in 2003. He is an Associate Professor of Computer Networks and Internet of Things and the Pro-Vice-Chancellor for Digital Technologies at the University of Salento. His research interests include RFID, IoT, WSN, and embedded systems. He has authored more than 180 scientific papers published in international journals and conferences. He is the Organizing Chair of some international symposia and workshops focused on the IoT.

MASSIMO DE VITTORIO (Senior Member, IEEE) is currently the Coordinator of the Center for Biomolecular Nanotechnologies, Istituto Italiano di Tecnologia, Lecce, Italy, and a Full Professor at Università del Salento, where he is a Lecturer of "Electronic and Photonic Devices" and "Nanotechnologies for Electronics" courses. He has been responsible for the Nanodevice Division, National Nanotechnology Laboratory (NNL), and CNR Istituto Nanoscience for over ten years. During his career, he has designed and coordinated micro and nanofabrication facilities with both backend and frontend technologies, with full prototyping and small/medium scale production capabilities. He has been a consultant for high-tech corporations and is a founder/advisor of four startup companies. He has authored 280 manuscripts in indexed journals, 70 conference proceedings, 14 patents, ten book chapters, and more than 60 invited/keynote talks at international conferences. His research interests include the development of science and technology applied to nanophotonics, nanoelectronics, and nano and micro electromechanical systems (NEMS/MEMS) for applications in the life sciences, energy, and ICT fields. He is a Senior Editor of the IEEE TRANSACTIONS ON NANOTECHNOLOGY Journal, a Board Member of the International Micro and Nanoengineering Society (iMNEs), and a member of the Editorial Board of the Journal Microelectronic Engineering.